Journal of Medicinal Chemistry

Article

pubs.acs.org/jmc

Identification and Characterization of Small Molecules as Potent and Specific EPAC2 Antagonists

Haijun Chen,[†] Tamara Tsalkova,[†,‡] Oleg G. Chepurny,[§] Fang C. Mei,[†,‡] George G. Holz,[§,∥] Xiaodong Cheng,*[,†,‡] and Jia Zhou*[,†]

[†]Department of Pharmacology and Toxicology and [‡]Sealy Center for Structural Biology and Molecular Biophysics, University of Texas Medical Branch, Galveston, Texas 77555, United States

[§]Department of Medicine and [∥]Department of Pharmacology, State University of New York (SUNY), Upstate Medical University, Syracuse, New York 13210, United States

Supporting Information

ABSTRACT: EPAC1 and EPAC2, two isoforms of exchange proteins directly activated by cAMP (EPAC), respond to the second messenger cAMP and regulate a wide variety of intracellular processes under physiological and pathophysiological circumstances. Herein, we report the chemical design, synthesis, and pharmacological characterization of three different scaffolds (diarylsulfones, *N*,*N*-diarylamines, and arylsulfonamides) as highly potent and selective antagonists of EPAC2. Several selective EPAC2 antagonists have been identified including **20i** (HJC0350), which has an apparent IC_{50} of 0.3 μM for competing with 8-NBD-cAMP binding of EPAC2 and is about 133-fold more potent than cAMP. Compounds **1** (ESI-05), **14c** (HJC0338), and **20i**, selected from each series, have exhibited no inhibition of EPAC1-mediated Rap1-GDP exchange activity at 25 μM, indicating that they are EPAC2-specific antagonists. Moreover, live-cell imaging studies using EPAC1, EPAC2, or PKA FRET sensor also demonstrate that **20i** functions as an EPAC2 specific antagonist.

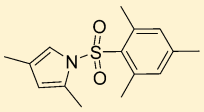

20i (HJC0350)

EPAC2: IC_{50} = 0.3 μM

EPAC1: No Effect

INTRODUCTION

Identification and development of small-molecule probes with high potency and specificity represent a major effort for chemical biologists to explore and validate the roles of the proteins in a broader biological context.[1] The most common and versatile second messenger, cyclic adenosine monophosphate (cAMP), regulates a striking number of physiological and pathophysiological processes through the signaling networks that interfere with many disease states including inflammatory disorders, immune deficiencies, and cancer.[2] Initially, the effects of cAMP were believed to be transduced by protein kinase A (PKA) and cAMP-gated ion channels. However, the contribution of more recently discovered cAMP target exchange proteins directly activated by cAMP (EPAC) is becoming more and more appreciated.[3−7] EPAC proteins are now assumed to be implicated in a number of cellular processes that researchers had previously thought to be associated only with PKA, including insulin secretion, neurotransmitter release, integrin-mediated cell adhesion, cell survival and apoptosis, gene transcription, and chromosomal integrity.[8−10] Therefore, advances in the understanding the role of EPAC proteins as regulators of cAMP-dependent signaling are critical for further elucidating the mechanism of cAMP signaling. cAMP analogues that selectively activate EPAC have been developed to help reveal the ability of EPAC to modulate ongoing physiological signaling.[11−13] Nevertheless, novel EPAC-specific antagonists are desperately needed as diverse approaches to help elucidation of the mechanisms by which cAMP fulfills its function via EPAC.[14,15] To this end, we direct our efforts on identification of novel small molecules as selective EPAC antagonists to probe the functions of EPAC in relevant signaling pathways and that act as potential therapeutics with unique targets.[16−18]

EPAC is a cAMP-activated guanine nucleotide exchange factor (cAMP-GEF) for the small GTP-binding proteins Rap1 and Rap2.[3,4] There are two isoforms of EPAC, EPAC1 and EPAC2, which are coded by two independent genes with distinct tissue distributions in mammals. EPAC1 is ubiquitously expressed in all tissues with high levels of expression in the kidney, while EPAC2 is detectable most notably in the central nervous system, adrenal gland, and pancreas. Given that EPAC1 and EPAC2 share extensive sequence homology, developing EPAC1- or EPAC2-specific antagonists with the capability of discriminating the functions of EPAC1 and EPAC2 is quite essential in this field.

To identify new chemical probes with high capability of specifically inhibiting EPAC, a Maybridge Hitfinder compound library of 14 400 structurally diverse small molecules has been screened using a fluorescence-based high-throughput screening (HTS) assay.[16−18] This assay was based on a fluorescent cyclic nucleotide analogue 8-NBD-cAMP, the binding of which to purified full-length EPAC2 protein could lead to a dose-dependent increase in fluorescent signal, while cAMP or EPAC2 antagonists could compete with their binding and decrease the fluorescent signal in a dose-dependent manner.[16] After analysis of the EPAC2 inhibition activity, some of the compounds screened from the library were applied to detect

Received: September 28, 2012
Published: January 3, 2013

   dx.doi.org/10.1021/jm3014162 | *J. Med. Chem.* 2013, 56, 952−962

their selectivity using a secondary functional assay that could evaluate their cAMP-mediated EPAC1 GEF activity in the purified recombinant full-length EPAC1 protein. Two HTS hits **1** (ESI-05) and **2** (ESI-10) have been identified (Figure 1),

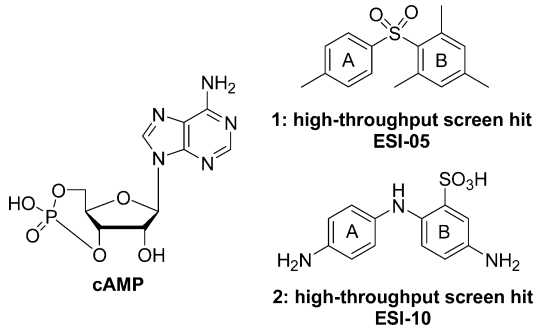

Figure 1. Structures of cAMP and HTS hits: **1** (ESI-05) and **2** (ESI-10).

which inhibit cAMP-mediated EPAC2 GEF activity with IC_{50} values of 0.5 and 18 μM, respectively. The hit compound **1** is exhibited as a selective antagonist of EPAC2 without apparent activity toward EPAC1, while **2** is not exclusively specific for EPAC2.[18b]

In continuation of our efforts to identify novel potent and EPAC-specific antagonists,[17] we have designed, synthesized, and characterized three different series of new molecules, namely, diarylsulfones, *N,N*-diarylamines, and arylsulfonamides based on the two HTS hits **1** and **2** as our lead molecules. Herein, we describe our findings on their potency and specificity as well as the structure–activity relationship (SAR) results of the new analogues.

RESULTS AND DISCUSSION

Chemistry. Our previous medicinal chemistry effort and molecular dockings have demonstrated that appropriate hydrophobic pharmacophores of the molecules play a crucial role for their potency and EPAC-isoform specificity.[17] Therefore, in our initial drug design and SAR studies, we have attempted to retain 2,4,6-trimethylphenyl ring of hit **1** as a privileged fragment to investigate the new molecules. As shown in Scheme 1, the diarylsulfone derivatives **5a–c** and **8a,b** were prepared via Friedel–Crafts sulfonylation of **3a–c** with 2,4,6-trimethylbenzene-1-sulfonyl chloride **4** or that of **7** with substituted benzenesulfonyl chlorides **6a,b** in 69–96% yields. The target compound **9** was obtained by Suzuki coupling reaction of **8a** with 2-fluoropyridine-5-boronic acid in the presence of Pd(dppf)Cl_2 catalyst in 70% yield. Generation of **10** was achieved in 92% yield by demethylation of **8b** using boron tribromide. Compounds **11a–d** were produced in 77–90% overall yields by Mitsunobu reaction of **10**, followed by subsequent Boc-deprotection with trifluoroacetic acid if necessary (e.g., **11c,d**).

The synthetic route to *N,N*-diarylamine derivatives is outlined in Scheme 2. *N,N*-Diarylamine analogues **14a–c** were prepared from substituted anilines **12a–c** by palladium-catalyzed cross-coupling with 2,4,6-mesityl bromide **13** in 62–93% yields. The cyclization reaction of α-bromoketone **15** with substituted thiourea **16** afforded *N*-phenylthiazoleamine **17** in 65% yield.

Scheme 3 illustrates the synthesis of diversely substituted arylsulfonamide analogues. Substituted pyrroles **18a,b** were

Scheme 1. Synthesis of the Diarylsulfone Scaffolds[a]

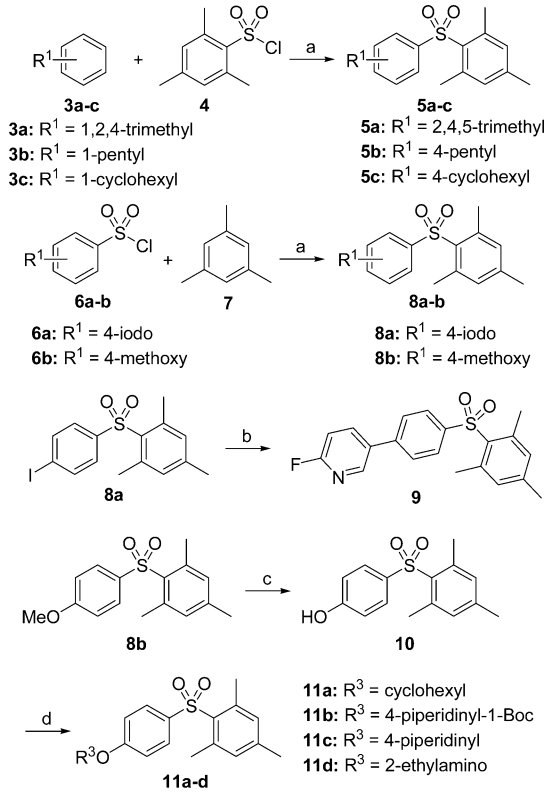

[a]Reagents and conditions: (a) $AlCl_3$, 25 °C, 69–96%; (b) Pd(dppf)-Cl_2, KOAc, $ArB(OH)_2$, THF/EtOH/H_2O, 80 °C, 70%; (c) BBr_3, DCM, 0–25 °C, 92%. (d) For **11a** and **11b**: DIAD, PPh_3, THF, 25 °C, 77–90%. For **11c** and **11d**: (i) DIAD, PPh_3, THF, 25 °C, 87–90%; (ii) TFA, DCM, 0 °C, 98–99%.

Scheme 2. Synthesis of the *N,N*-Diarylamine Scaffold[a]

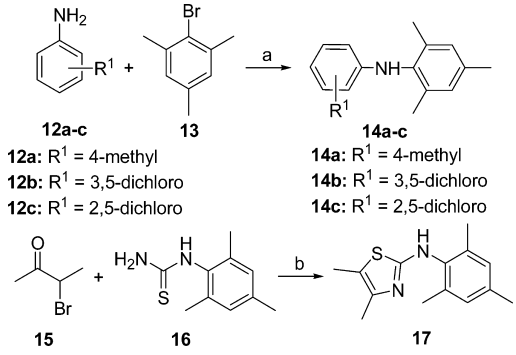

[a]Reagents and conditions: (a) $Pd_2(dba)_3$, NaO^{t}Bu, (±)-BINAP, toluene, 120 °C, 62–93%; (b) EtOH, reflux, 65%.

treated with various sulfonyl chlorides **19a–h** in the presence of 60% NaH as base to give the corresponding arylsulfonamides **20a–i** in 30–96% yields. The synthesis of indole and azaindole derivatives **22a–c** and **24a–d** was accomplished by the treatment of various indoles **21a,b** or azaindoles **23a–d** with 2,4,6-trimethylbenzene-1-sulfonyl chloride **4** in a similar fashion. The indole ester **22b** was saponified to generate the carboxylic acid **22c** in 66% yield.

In Vitro Evaluation of EPAC2 Inhibition. All compounds have been evaluated for their inhibitory activity against the recombinant fusion protein EPAC2 using 8-NBD-cAMP as the

dx.doi.org/10.1021/jm3014162 | J. Med. Chem. 2013, 56, 952–962

Scheme 3. Synthesis of the Arylsulfonamide Scaffold[a]

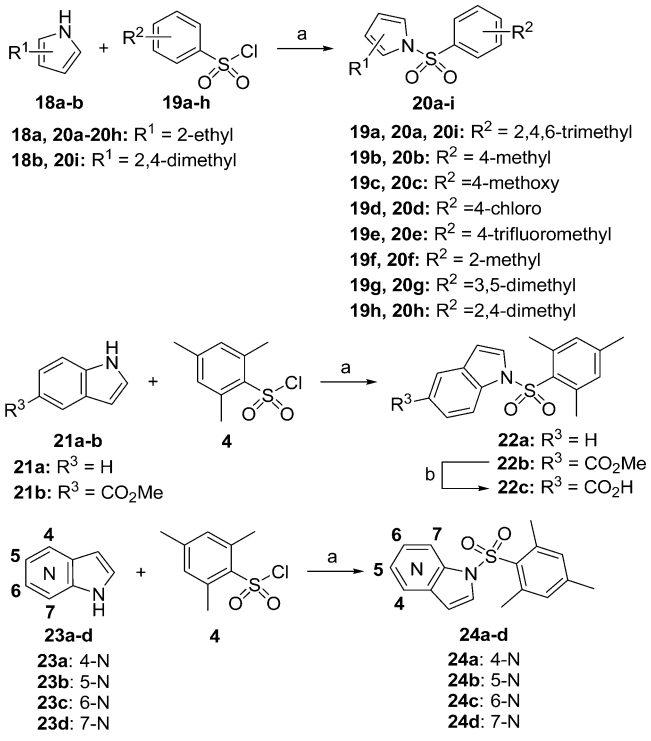

[a]Reagents and conditions: (a) 60% NaH, THF, 0−25 °C, 30−96%; (b) 2 N LiOH/H_2O, MeOH/H_2O, 25 °C, 66%.

artificial substrate to determine IC_{50} values, while cAMP competes with 8-NBD-cAMP in binding EPAC2 with an IC_{50} of 40 μM.[16] Table 1 shows apparent IC_{50} values of the diarylsulfones and *N*,*N*-diarylamine scaffolds for competing with 8-NBD-cAMP in binding EPAC2. Among these new diarylsulfone analogues, compound **5a** is the most potent antagonist with an IC_{50} of 0.7 μM. When one aryl ring of the diarylsulfones is substituted with too bulky groups including 4-pentyl, 4-cyclohexyl, and 4-*O*-piperidinyl, these compounds such as **5b−c**, **9**, and **11a−d** display very low to no activity. When the methyl group in one ring of hit **1** is replaced by iodo, methoxy, or hydroxyl, compounds **8a**,**b** and **10** exhibit a slightly lower potency with IC_{50} of 4, 1.9, and 13.5 μM, respectively. Among *N*,*N*-diarylamine derivatives, compound **14a** is a new analogue of hit **2** with the 4-amino group of one phenyl ring replaced by the 4-methyl substituent and the 5-amino-benzenesulfonic acid moiety replaced by the 2,4,6-trimethyl-phenyl fragment. **14a** demonstrates a substantially enhanced activity with an IC_{50} of 3.8 μM when compared with the hit lead **2**. Interestingly, analogues **14b**,**c** with the 3,5-dichloro or 2,5-dichloro exhibit a significantly better potency with IC_{50} values of 0.9 and 0.4 μM, respectively, than the 4-methyl derivative **14a**. Compound **17** containing a thiazole ring as one of the aromatic moieties was also explored and was found to have no activity.

On the basis of the structural features of hits **1** and **2** as well as the preliminary SAR results from the above efforts, we have designed and investigated a series of arylsulfonamides as a new chemical entity of EPAC2 antagonists. The findings of the arylsulfonamide analogues are summarized in Table 2. Compound **20a** with a 2-ethylpyrrole moiety displays a high potency of EPAC2 inhibition with an IC_{50} of 0.5 μM. Analogues **20b−h** with 2,4,6-trimethylphenyl moiety replaced by other substituted phenyl groups exhibit apparently dampened activities in comparison with **20a**. Interestingly, the 4-trifluoromethyl substituent on the phenyl ring of analogue

Table 1. Apparent IC_{50} Values of the Diarylsulfones and *N*,*N*-Diarylamine Scaffolds for Competing with 8-NBD-cAMP in Binding EPAC2

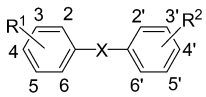

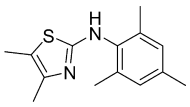
17

compd	R^1	R^2	X	IC_{50} (μM)	relative potency (RA)[a]
cAMP				40	1
1	4-methyl	2′,4′,6′-trimethyl	SO_2	0.5	80
2	4-NH_2	2′-SO_3H-4′-NH_2	NH	18	2.2
5a	2,4,5-trimethyl	2′,4′,6′-trimethyl	SO_2	0.7	57.1
5b	4-pentyl	2′,4′,6′-trimethyl	SO_2	>300	<0.13
5c	4-cyclohexyl	2′,4′,6′-trimethyl	SO_2	>300	<0.13
8a	4-iodo	2′,4′,6′-trimethyl	SO_2	4	10
8b	4-methoxy	2′,4′,6′-trimethyl	SO_2	1.9	21.1
9	4-(2-fluoro-5-pyridinyl)	2′,4′,6′-trimethyl	SO_2	>300	<0.13
10	4-hydroxyl	2′,4′,6′-trimethyl	SO_2	13.5	3.0
11a	4-*O*-cyclohexyl	2′,4′,6′-trimethyl	SO_2	>300	<0.13
11b	4-*O*-piperidinyl-1-Boc	2′,4′,6′-trimethyl	SO_2	>300	<0.13
11c	4-*O*-piperidinyl	2′,4′,6′-trimethyl	SO_2	>300	<0.13
11d	4-*O*-2-ethylamino	2′,4′,6′-trimethyl	SO_2	>300	<0.13
14a	4-methyl	2′,4′,6′-trimethyl	NH	3.8	10.5
14b	3,5-dichloro	2′,4′,6′-trimethyl	NH	0.9	44.4
14c	2,5-dichloro	2′,4′,6′-trimethyl	NH	0.4	100
17			NH	>300	<0.13

[a]RA = $IC_{50,cAMP}$/ $IC_{50,compound}$.

dx.doi.org/10.1021/jm3014162 | *J. Med. Chem.* 2013, 56, 952−962

Table 2. Apparent IC_{50} Values of the Arylsulfonamide Scaffold for Competing with 8-NBD-cAMP in Binding EPAC2

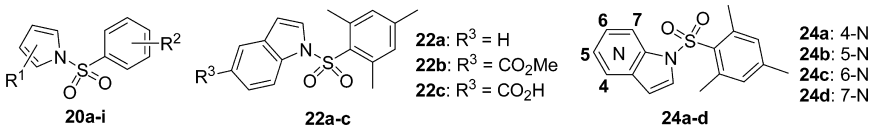

compd	R^1	R^2	IC_{50} (μM)	relative potency (RA)[a]	compd	IC_{50} (μM)	relative potency (RA)[a]
20a	2-ethyl	2,4,6-trimethyl	0.5	80	**22a**	1.2	33.3
20b	2-ethyl	4-methyl	4	10	**22b**	>300	<0.13
20c	2-ethyl	4-methoxy	8	5	**22c**	10.8	3.7
20d	2-ethyl	4-chloro	8	5	**24a**	3.8	10.5
20e	2-ethyl	4-trifluoromethyl	>300	<0.13	**24b**	8.9	4.5
20f	2-ethyl	2-methyl	5.3	7.5	**24c**	12.6	3.2
20g	2-ethyl	3,5-dimethyl	4.7	8.5	**24d**	2.4	16.7
20h	2-ethyl	2,4-dimethyl	1.3	30.8	cAMP	40	1
20i	2,4-dimethyl	2,4,6-trimethyl	0.3	133			

[a]RA = $IC_{50,cAMP}$/ $IC_{50,compound}$.

20e results in a dramatic loss of EPAC inhibitory activity. Compound **20i** bearing the 2,4-dimethylpyrrole fragment displays a remarkable activity with an IC_{50} of 0.3 μM, which is about 133-fold more potent than cAMP (Table 2, Figure 2).

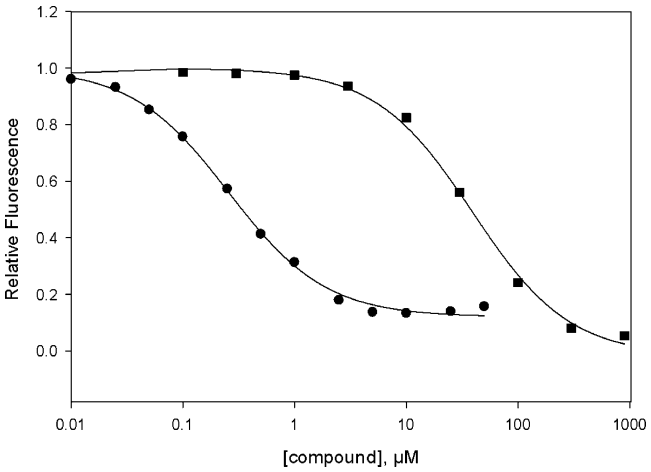

Figure 2. Relative potency of EPAC2 antagonist **20i** (HJC0350), showing dose-dependent competition of EPAC2 antagonists with 8-NBD-cAMP in binding to EPAC2: closed circles, **20i**; closed squares, cAMP.

Analogues **22a–c** and **24a–d** have been investigated to replace the pyrrole scaffold with the indole or azaindole moieties. Among these new molecules, the indole analogue **22a** and the 7-azaindole analogue **24d** display an almost retained activity of EPAC2 inhibition in contrast with pyrrole derivatives. Analogues **22c** and **24a–c** are less active with a moderate potency. An ester group on indole ring of **22b** results in a dramatic loss of activity, while the saponification of the ester **22b** to carboxylic acid **22c** can significantly regain the inhibitory activity of EPAC2. Taken together, the preliminary SAR results support that appropriate hydrophobic pharmacophores of the molecules play a crucial role for their activity targeting the EPAC proteins, and more potent ligands may be achieved through further systematic and extensive structural optimizations.

Selectivity for EPAC2. To investigate the EPAC-isoform specificity, the inhibitory potencies of three most potent compounds **1**, **14c**, and **20i** selected from three different scaffolds have been evaluated in suppressing cAMP-mediated EPAC1 and EPAC2 GEF activities using purified recombinant full-length EPAC1 and EPAC2 proteins (Figure 3).[16,19,20] These three analogues have been shown to be able to inhibit EPAC2 GEF activity to basal levels at 25 μM in the presence of equal concentration of cAMP. All of these compounds were found not to inhibit EPAC1-mediated Rap1-GDP exchange activity at 25 μM in the presence of equal concentration of cAMP, indicating that they are EPAC2-specific antagonists. To further investigate their specificity for EPAC over PKA, we performed counterscreening assays that measure type I and type II PKA holoenzyme activities.[16,21,22] All these analogues have demonstrated that they do not significantly alter cAMP-induced type I and type II PKA holoenzymes activation at 25 μM, while the selective PKA inhibitor H89, the positive control, blocked the type I or II PKA activities completely. These results suggest that compounds **1**, **14c** (HJC0338), and **20i** (HJC0350) are EPAC2-specific antagonists that selectively block cAMP-induced EPAC2 activation but do not inhibit cAMP-mediated PKA activation. It should be emphasized that while these compounds exert no activity toward PKA, their pharmacological properties should be further evaluated to ensure that they do not disrupt other components of the cyclic nucleotide signaling pathways, such as the cyclic-nucleotide regulated ion channels (CNG and HCN channels), phosphodiesterases, or adenylyl cyclases.

To test whether **20i** is capable of modulating EPAC activation in living cells and to further validate that **20i** is an EPAC2 isoform-specific antagonist, we tested the compound using HEK293 cells stably expressing an EPAC2- or EPAC1-based fluorescence resonance energy transfer (FRET) sensor, EPAC2-FL or EPAC1-FL.[23] As expected, stimulation of HEK293/EPAC2-FL cells by 8-(4-chlorophenylthio)-2′-*O*-methyladenosine 3′,5′-cyclic monophosphate acetoxymethyl ester (007-AM), a membrane permeable EPAC selective cAMP analogue, led to a decrease of FRET measured as an increase of the 485/535 nm FRET ratio (Figure 4A). Pretreatment of HEK293/EPAC2-FL cells with 10 μM **20i** fully blocked the 007-AM induced decrease of FRET (Figure 4B). In contrast, **20i** was found to be incapable of blocking the 007-AM induced decrease of FRET changes in HEK293/EPAC1-FL (Figure 4C and Figure 4D). By use of HEK293 cells stably expressing the PKA sensor AKAR3,[24] it was also possible to demonstrate the stimulatory action of 8-Br-cAMP-AM at

dx.doi.org/10.1021/jm3014162 | J. Med. Chem. 2013, 56, 952–962

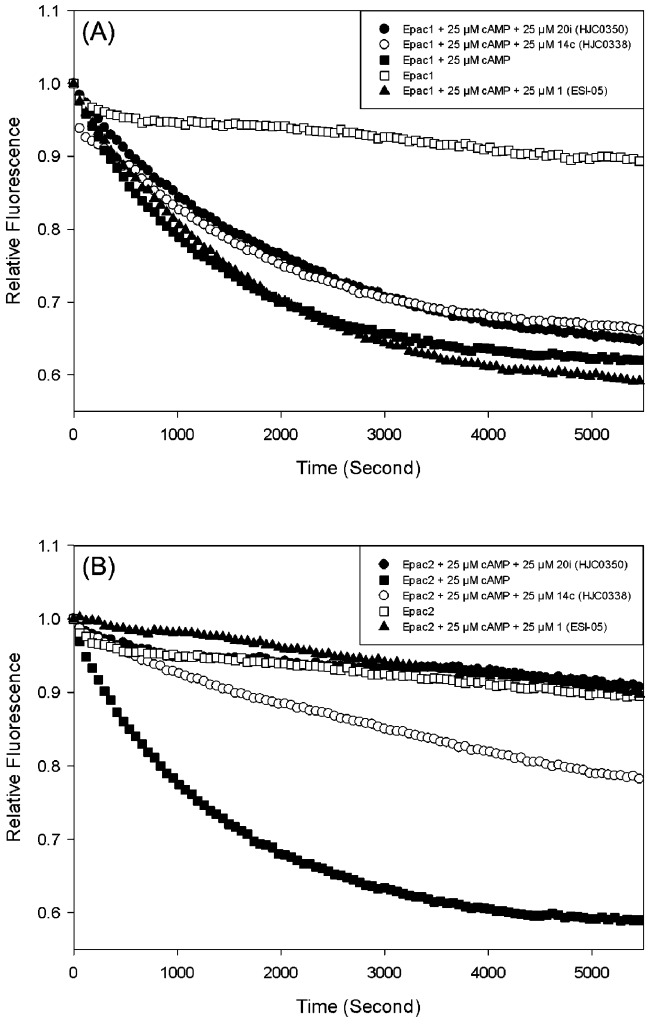

Figure 3. Specificity of EPAC antagonists **1**, **14c**, and **20i**. (A) cAMP-mediated EPAC1 GEF activity measured in the presence or absence of EPAC antagonists: open squares, EPAC1 alone; closed squares, EPAC1 in the presence of 25 μM cAMP; closed triangles up, EPAC1 with 25 μM cAMP and 25 μM **1**; open circles, EPAC1 with 25 μM cAMP and 25 μM **14c**; closed circles, EPAC1 with 25 μM cAMP and 25 μM **20i**. (B) cAMP-mediated EPAC2 GEF activity measured in the presence or absence of EPAC antagonists: open squares, EPAC2 alone; closed squares, EPAC2 in the presence of 25 μM cAMP; closed triangles up, EPAC2 with 25 μM cAMP and 25 μM **1**; open circles, EPAC2 with 25 μM cAMP and 25 μM **14c**; closed circles, EPAC2 with 25 μM cAMP and 25 μM **20i**.

PKA, as measured as an increase FRET with a corresponding decrease of the 485/535 nm FRET ratio (Figure 5A). This action of 8-Br-cAMP-AM to activate PKA was not inhibited by **20i** (Figure 5B). These live-cell results are in complete agreement with our biochemical data and further validate that **20i** is an effective EPAC2-isoform specific antagonist.

CONCLUSION

In summary, this work presents three series of new molecules that exhibit outstanding selectivity and potency for the inhibition of EPAC2 through a preliminary hit-to-lead optimization process. Analogues **14c** and **20i** have been identified as the most potent EPAC2-specific antagonists with IC_{50} values of 0.4 and 0.3 μM, which are about 100- and 133-fold more potent than cAMP, respectively. Accumulating studies support that EPAC proteins may represent promising targets for the design of new therapies for various human disorders such as diabetes, heart disease, and cancer.[25−29] Therefore, these compounds may not only be valuable pharmacological tools to explore physiological and pathological processes related to signaling pathways that are regulated by EPAC proteins but also have great potential to be developed as novel molecular therapeutics for relevant human diseases. Further structural optimization of these scaffolds based upon our SAR findings and in vivo pharmacological evaluation of selected EPAC antagonists in disease models are currently underway.

EXPERIMENTAL SECTION

General Chemistry Information. All commercially available starting materials and solvents were reagent grade and used without further purification. Reactions were performed under a nitrogen atmosphere in dry glassware with magnetic stirring. Preparative column chromatography was performed using silica gel 60, particle size 0.063−0.200 mm (70−230 mesh, flash). Analytical TLC was carried out employing silica gel 60 F254 plates (Merck, Darmstadt, Germany). Visualization of the developed chromatograms was performed with detection by UV (254 nm). NMR spectra were recorded on a Bruker 600 (^{1}H, 600 MHz; ^{13}C, 150 MHz) spectrometer. ^{1}H and ^{13}C NMR spectra were recorded with TMS as an internal reference. Chemical shifts were expressed in ppm, and J values were given in Hz. High-resolution mass spectra were obtained using a Thermo Fisher LTQ Orbitrap Elite mass spectrometer. Parameters include the following: nano ESI spray voltage was 1.8 kV; capillary temperature was 275 °C, and the resolution was 60 000; ionization was achieved by positive mode. Melting points were measured on a Thermo Scientific electrothermal digital melting point apparatus and uncorrected. Purities of final compounds were established by analytical HPLC, which was carried out on a Shimadzu HPLC system (model CBM-20A LC-20AD SPD-20A UV/vis). HPLC analysis conditions were as follows: Waters μBondapak C18 (300 mm × 3.9 mm); flow rate, 0.5 mL/min; UV detection at 270 and 254 nm; linear gradient from 10% acetonitrile in water to 100% acetonitrile in water in 20 min followed by 30 min of the last-named solvent (for **11c** and **11d**, the same mobile phase with 0.1% TFA). All biologically evaluated compounds are >95% pure.

1,3,5-Trimethyl-2-(2,4,5-trimethylbenzenesulfonyl)benzene (5a). A mixture of mesitylsulfonyl chloride (219 mg, 1.0 mmol), 1,2,4-trimethylbenzene (125 mg, 1.05 mmol), and $AlCl_3$ (266 mg, 2.0 mmol) in DCM (5 mL) was stirred for 2 h at room temperature. The mixture was then poured into 10 mL of 5% HCl (aq) and extracted by DCM (30 mL). The organic phase was washed by aqueous $KHCO_3$ solution, brine and dried over anhydrous Na_2SO_4. The resulting solution was evaporated, and the residue was purified by silica gel column chromatography (hexane/EtOAc = 10/1) to give the desired product as a white solid (290 mg, 96%): mp 147−148 °C; HPLC purity 98.4% (t_R = 25.33 min). ^{1}H NMR (600 MHz, DMSO-d_6) δ 7.70 (s, 1H), 7.11 (s, 1H), 7.05 (s, 2H), 2.38 (s, 6H), 2.27 (s, 6H), 2.25 (s, 3H), 2.07 (s, 3H). ^{13}C NMR (150 MHz, DMSO-d_6) δ 143.0, 142.3, 138.5, 138.4, 134.4, 134.3, 133.7, 133.3, 132.0, 128.2, 21.8, 20.5, 19.1, 18.9, 17.8. HRMS (ESI) calcd for $C_{18}H_{23}O_2S$ 303.1413 $(M + H)^+$, found 303.1407.

1,3,5-Trimethyl-2-(4-pentylbenzenesulfonyl)benzene (5b). Compound **5b** was prepared in 90% yield by a procedure similar to that used to prepare compound **5a**. The title compound was obtained as a pale yellow oil. HPLC purity 97.2% (t_R = 26.16 min). ^{1}H NMR (600 MHz, $CDCl_3$) δ 7.68 (d, 2H, J = 7.2 Hz), 7.25 (d, 2H, J = 6.6 Hz), 6.93 (s, 2H), 2.63 (t, 2H, J = 7.2 Hz), 2.49 (s, 6H), 2.28 (s, 3H), 1.57−1.62 (m, 2H), 1.28−1.32 (m, 4H), 0.88 (t, 2H, J = 6.6 Hz). ^{13}C NMR (150 MHz, $CDCl_3$) δ 148.4, 143.3, 140.9, 140.1, 134.3, 132.3, 128.9, 126.4, 35.9, 31.5, 30.8, 22.9, 22.6, 21.1, 14.1. HRMS (ESI) calcd for $C_{20}H_{27}O_2S$ 331.1726 $(M + H)^+$, found 331.1734.

dx.doi.org/10.1021/jm3014162 | J. Med. Chem. 2013, 56, 952−962

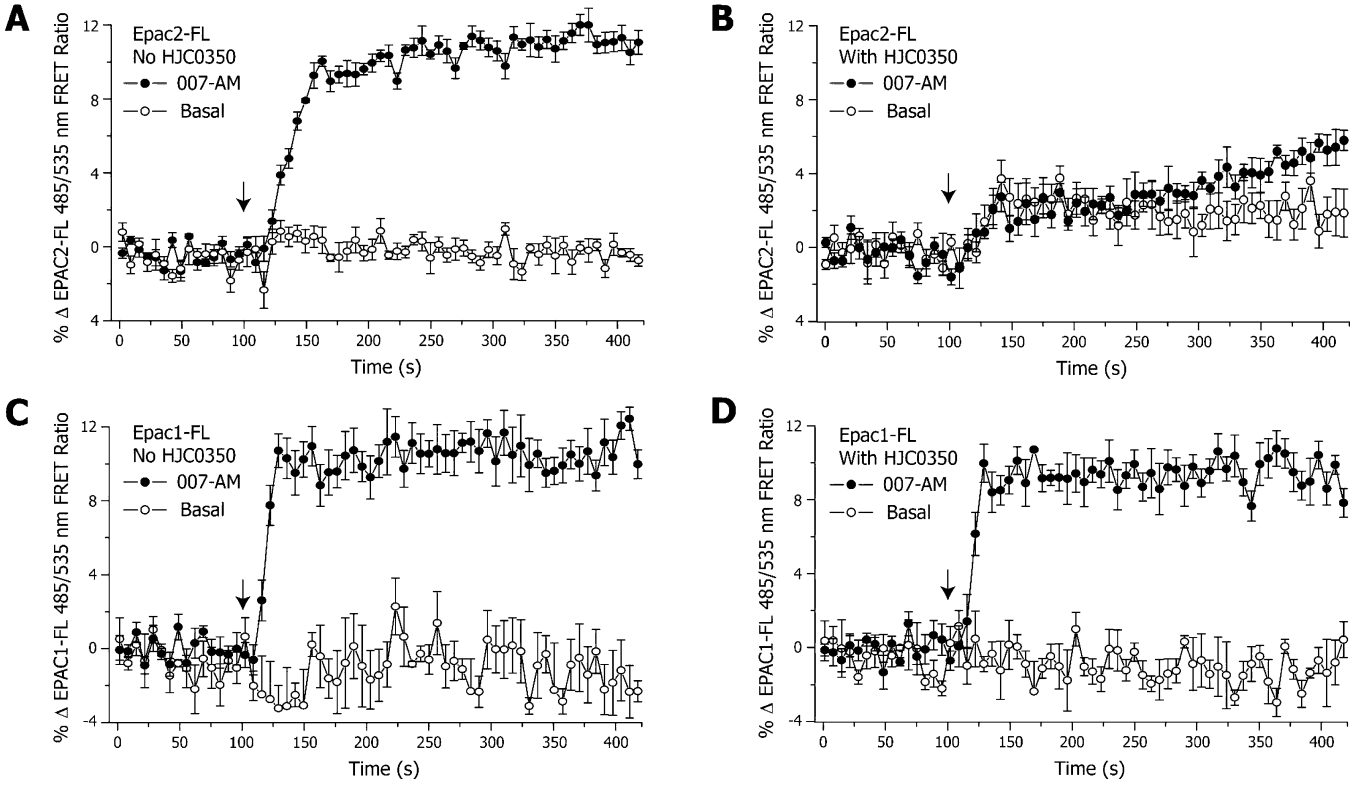

Figure 4. Effects of **20i** on 007-AM mediated cellular activation of EPAC. For HEK293 cells stable expression EPAC2-FL (A, B) or EPAC1-FL (C, D), it was demonstrated that 10 μM **20i** blocked EPAC2 but not EPAC1 activation in response to 10 μM 007-AM.

2-(4-Cyclohexylbenzenesulfonyl)-1,3,5-trimethylbenzene (5c). Compound **5c** was prepared in 75% yield by a procedure similar to that used to prepare compound **5a**. The title compound was obtained as a white solid (mp 102−103 °C). HPLC purity 99.8% (t_R = 26.29 min). ^{1}H NMR (600 MHz, $CDCl_3$) δ 7.69 (d, 2H, J = 8.4 Hz), 7.27 (d, 2H, J = 8.4 Hz), 6.93 (s, 2H), 2.60 (s, 6H), 2.52−2.55 (m, 1H), 2.27 (s, 3H), 1.82−1.83 (m, 4H), 1.73−1.75 (m, 1H), 1.34−1.41 (m, 4H), 1.22−1.26 (m, 1H). ^{13}C NMR (150 MHz, $CDCl_3$) δ 153.3, 143.2, 141.0, 140.0, 134.3, 132.2, 127.4, 126.4, 44.6, 34.2, 26.7, 26.0, 22.9, 21.0. HRMS (ESI) calcd for $C_{21}H_{27}O_2S$ 343.1726 (M + H)$^+$, found 343.1730.

2-(4-Iodobenzenesulfonyl)-1,3,5-trimethylbenzene (8a). A mixture of 4-iodobenzenesulfonyl chloride (302 mg, 1.0 mmol), mesitylene (120 mg, 1.0 mmol), and $AlCl_3$ (150 mg, 1.2 mmol) in DCM (5 mL) was stirred for 2 h at room temperature. The mixture was then poured into 10 mL of 5% HCl (aq) and extracted by DCM (30 mL). The organic phase was washed by aqueous $KHCO_3$, brine and dried over anhydrous Na_2SO_4. The resulting solution was evaporated, and the residue was purified by silica gel column chromatography (hexane/EtOAc = 10/1) to give the desired product (266 mg, 69%) as a white solid (mp 123−124 °C). HPLC purity 96.0% (t_R = 23.82 min). ^{1}H NMR (600 MHz, $CDCl_3$) δ 7.82 (d, 2H, J = 8.4 Hz), 7.48 (d, 2H, J = 7.8 Hz), 6.95 (s, 2H), 2.58 (s, 6H), 2.30 (s, 3H). ^{13}C NMR (150 MHz, $CDCl_3$) δ 143.9, 143.4, 140.2, 138.3, 133.5, 132.5, 127.8, 100.0, 23.0, 21.2. HRMS (ESI) calcd for $C_{15}H_{16}IO_2S$ 386.9910 (M + H)$^+$, found 386.9915.

2-(4-Methoxybenzenesulfonyl)-1,3,5-trimethylbenzene (8b). Compound **8b** was prepared in 86% yield by a procedure similar to that used to prepare compound **8a**. The title compound was obtained as a white solid (mp 132−133 °C). HPLC purity 98.9% (t_R = 21.80 min). ^{1}H NMR (600 MHz, $CDCl_3$) δ 7.72 (d, 2H, J = 8.4 Hz), 6.93 (d, 2H, J = 7.2 Hz), 6.92 (s, 2H), 3.84 (s, 3H), 2.60 (s, 6H), 2.28 (s, 3H). ^{13}C NMR (150 MHz, $CDCl_3$) δ 162.9, 143.2, 140.0, 135.4, 134.7, 132.3, 128.6, 114.2, 55.7, 23.0, 21.1. HRMS (ESI) calcd for $C_{16}H_{19}O_3S$ 291.1049 (M + H)$^+$, found 291.1056.

2-Fluoro-5-[4-(2,4,6-trimethylbenzenesulfonyl)phenyl]-pyridine (9). To a solution of **8a** (77 mg, 0.2 mmol) and 2-fluoropyridine-5-boronic acid (28 mg, 0.2 mmol) in THF/EtOH/H_2O (1 mL/1 mL/1 mL) were added KOAc (59 mg, 0.6 mmol) and then $Pd(dppf)Cl_2$ (16 mg, 0.02 mmol). The resulting mixture was deoxygenated via five vacuum/N_2-refill cycles. The mixture was stirred at 80 °C for 18 h and was then concentrated under vacuum. The residue was partitioned between EtOAc (50 mL) and H_2O (20 mL). The organic layer was separated and washed with brine (10 mL), dried over anhydrous Na_2SO_4, filtered, and concentrated to give an oily residue. This residue was purified with silica gel column (hexane/EtOAc = 3/1) to obtain **9** (50 mg, 70%) as a red solid (mp 150−151 °C). HPLC purity 95.1% (t_R = 22.50 min). ^{1}H NMR (600 MHz, $CDCl_3$) δ 8.39−8.41 (m, 1H), 7.95−7.98 (m, 1H), 7.88 (d, 2H, J = 8.4 Hz), 7.62−7.65 (m, 2H), 7.03 (d, 1H, J = 8.4 Hz), 6.96 (s, 2H), 2.61 (s, 6H), 2.30 (s, 3H). ^{13}C NMR (150 MHz, $CDCl_3$) δ 164.5, 162.9, 146.3, 143.8, 143.3, 141.0, 140.2, 140.1, 133.6, 133.2, 132.4, 127.6, 127.2, 110.1, 109.9, 23.0, 21.1. HRMS (ESI) calcd for $C_{20}H_{19}FNO_2S$ 356.1115 (M + H)$^+$, found 356.1120.

4-(2,4,6-Trimethylbenzenesulfonyl)phenol (10). To a solution of **8b** (350 mg, 1.2 mmol) in 10 mL of DCM was added 1 N BBr_3/DCM (1.45 mL, 1.45 mmol) at 0 °C. The resulting mixture was stirred at room temperature for 16 h. The solution was diluted with EtOAc (50 mL), washed with H_2O (10 mL) and brine (10 mL). The organic layer was dried over anhydrous Na_2SO_4 and then concentrated under reduced pressure. The residue was purified by silica gel column chromatography (hexane/EtOAc = 3/1) to give the desired product (306 mg, 92%) as a white solid (mp 180−181 °C). HPLC purity 99.4% (t_R = 19.46 min). ^{1}H NMR (600 MHz, $CDCl_3$) δ 7.64 (d, 2H, J = 8.4 Hz), 6.93 (s, 2H), 6.86 (d, 2H, J = 8.4 Hz), 6.23 (bs, 1H), 2.58 (s, 6H), 2.29 (s, 3H). ^{13}C NMR (150 MHz, $CDCl_3$) δ 160.0, 143.4, 140.0, 135.1, 134.4, 132.4, 128.8, 115.8, 23.0, 21.1. HRMS (ESI) calcd for $C_{15}H_{17}O_3S$ 277.0893 (M + H)$^+$, found 277.0898.

2-(4-Cyclohexyloxybenzenesulfonyl)-1,3,5-trimethylbenzene (11a). To a solution of **10** (50 mg, 0.18 mmol) and Ph_3P (58 mg, 0.22 mmol) in THF (5 mL) was added cyclohexanol (36 mg, 0.36

dx.doi.org/10.1021/jm3014162 | J. Med. Chem. 2013, 56, 952−962

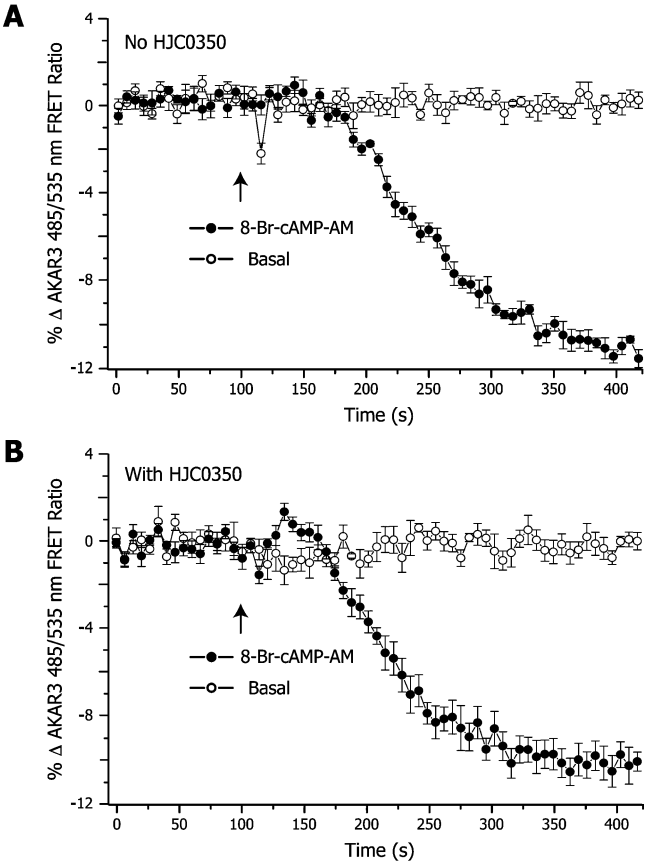

Figure 5. Effects of **20i** on 8-Br-cAMP-AM mediated cellular activation of PKA. For HEK293 cells stable expression AKAR3, it was demonstrated that 10 μM **20i** did not affect PKA activation in response to 10 μM 8-Br-cAMP-AM.

mmol) and DIAD (44 mg, 0.22 mmol). The reaction mixture was stirred at room temperature for 16 h, and then it was partitioned between EtOAc (50 mL) and H_2O (20 mL). The organic layer was washed with brine (10 mL), dried with anhydrous Na_2SO_4, and concentrated to give the crude product. This residue was purified with silica gel column (hexane/EtOAc = 7/1) to afford the desired product as a colorless oil (50 mg, 77%). HPLC purity 99.7% (t_R = 25.64 min). ^{1}H NMR (600 MHz, $CDCl_3$) δ 7.69 (d, 2H, J = 7.2 Hz), 6.91 (s, 2H), 6.91 (d, 2H, J = 6.6 Hz), 4.30 (s, 1H), 2.60 (s, 6H), 2.27 (s, 3H), 1.93−195 (m, 2H), 1.75−1.77 (m, 2H), 1.47−1.57 (m, 3H), 1.29−1.39 (m, 3H). ^{13}C NMR (150 MHz, $CDCl_3$) δ 161.4, 143.1, 139.9, 134.8, 134.8, 132.3, 128.6, 115.6, 75.8, 31.6, 25.6, 23.7, 23.0, 21.1. HRMS (ESI) calcd for $C_{21}H_{27}O_3S$ 359.1675 (M + H)$^+$, found 359.1680.

4-[4-(2,4,6-Trimethylbenzenesulfonyl)phenoxy]piperidine-1-carboxylic Acid *tert*-Butyl Ester (11b). Compound **11b** was prepared in 90% yield by a procedure similar to that used to prepare compound **11a**. The title compound was obtained as a colorless oil. HPLC purity 99.9% (t_R = 24.54 min). ^{1}H NMR (600 MHz, $CDCl_3$) δ 7.71 (d, 2H, J = 9.0 Hz), 6.93 (s, 2H), 6.91 (d, 2H, J = 8.4 Hz), 4.52−4.54 (m, 1H), 3.65−3.69 (m, 2H), 3.33−3.37 (m, 2H), 2.60 (s, 6H), 2.29 (s, 3H), 1.90−1.93 (m, 2H), 1.73−1.77 (m, 2H), 1.46 (s, 9H).

4-[4-(2,4,6-Trimethylbenzenesulfonyl)phenoxy]piperidine (11c). To a solution of **11b** (128 mg, 0.28 mmol) in DCM (5 mL) was added TFA (1 mL) at 0 °C. The mixture was stirred at 0 °C for 1 h. The reaction mixture was concentrated, and the residue was partitioned between EtOAc (50 mL) and 1 N $NaHCO_3$ (10 mL). The organic layer was washed with brine (10 mL), dried with anhydrous Na_2SO_4, and concentrated to give the crude product. This residue was purified with silica gel column (DCM/MeOH = 10/1) to provide **11c** (100 mg, 99%) as a white solid (mp 95−97 °C). HPLC purity 99.5% (t_R = 17.63 min). ^{1}H NMR (600 MHz, $CDCl_3$) δ 8.55 (bs, 1H), 7.70 (d, 2H, J = 7.2 Hz), 6.92 (d, 2H, J = 9.0 Hz), 6.91 (s, 2H), 4.67 (s, 1H), 3.28 (t, 2H, J = 8.4 Hz), 3.12−3.14 (m, 2H), 2.57 (s, 6H), 2.27 (s, 3H), 2.17 (t, 2H, J = 7.8 Hz), 2.02−2.04 (m, 2H). ^{13}C NMR (150 MHz, $CDCl_3$) δ 159.8, 143.4, 139.8, 136.1, 134.2, 132.3, 128.7, 115.6, 68.9, 40.2, 27.2, 22.9, 21.0. HRMS (ESI) calcd for $C_{20}H_{26}NO_3S$ 360.1628 (M + H)$^+$, found 360.1631.

2-[4-(2,4,6-Trimethylbenzenesulfonyl)phenoxy]ethylamine (11d). Compound **11d** was prepared in 85% yield (two steps) by a procedure similar to that used to prepare compounds **11a** and **11c**. The title compound was obtained a pale red oil. HPLC purity 97.7% (t_R = 16.68 min). ^{1}H NMR (600 MHz, $CDCl_3$) δ7.64 (d, 2H, J = 7.2 Hz), 6.89 (s, 2H), 6.88 (d, 2H, J = 7.2 Hz), 5.40−5.48 (bs, 2H), 4.02−4.03 (m, 2H), 3.10−3.12 (m, 2H), 2.52 (s, 6H), 2.23 (s, 3H). ^{13}C NMR (150 MHz, $CDCl_3$) δ 161.6, 143.4, 139.8, 135.7, 134.2, 132.3, 128.5, 114.7, 67.1, 40.0, 22.8, 21.1. HRMS (ESI) calcd for $C_{17}H_{22}NO_3S$ 320.1315 (M + H)$^+$, found 320.1319.

***p*-Tolyl-(2,4,6-trimethylphenyl)amine (14a).** NaO^{t}Bu (115 mg, 1.2 mmol), $Pd_2(dba)_3$ (92 mg, 0.1 mmol), and (±)-BINAP (124 mg, 0.2 mmol) were placed into a flask and dissolved into distilled toluene (5 mL). To this solution were added mesityl bromide (995 mg, 5.0 mmol) and *p*-tolylamine (107 mg, 1.0 mmol) dropwise with stirring at room temperature, and the mixture was refluxed at 120 °C for 24 h. After the mixture was cooled, 10 mL of 5% HCl (aq) was added and extracted with EtOAc (50 mL). The combined organic layer was washed with $NaHCO_3$ and dried over anhydrous Na_2SO_4, filtered, and concentrated in vacuo. The residue was purified by silica gel column chromatography (hexane/EtOAc = 10/1) to give the desired product as a pale yellow oil (210 mg, 93%). HPLC purity 99.4% (t_R = 24.58 min). ^{1}H NMR (600 MHz, $CDCl_3$) δ 7.11 (d, 2H, J = 7.8 Hz), 7.09 (s, 2H), 6.57 (d, 2H, J = 7.8 Hz), 5.12 (s, 1H), 2.47 (s, 3H), 2.40 (s, 3H), 2.33 (s, 6H). ^{13}C NMR (150 MHz, $CDCl_3$) δ 144.4, 136.1, 135.7, 135.1, 129.8, 129.3, 127.1, 113.5, 21.0, 20.5, 18.3. HRMS (ESI) calcd for $C_{16}H_{20}N$ 226.1590 (M + H)$^+$, found 226.1593.

(3,5-Dichlorophenyl)-(2,4,6-trimethylphenyl)amine (14b). Compound **14b** was prepared in 68% yield by a procedure similar to that used to prepare compound **14a**. The title compound was obtained as a pale yellow solid (mp 99−100 °C). HPLC purity 98.8% (t_R = 27.53 min). ^{1}H NMR (600 MHz, $CDCl_3$) δ 7.00 (s, 2H), 6.73 (s, 1H), 6.37 (s, 2H), 5.21 (s, 1H), 2.36 (s, 3H), 2.20 (s, 6H). ^{13}C NMR (150 MHz, $CDCl_3$) δ 148.8, 136.7, 136.4, 135.7, 133.9, 129.6, 117.7, 111.3, 21.0, 18.2. HRMS (ESI) calcd for $C_{15}H_{16}Cl_2N$ 280.0654 (M + H)$^+$, found 280.0653.

(2,5-Dichlorophenyl)-(2,4,6-trimethylphenyl)amine (14c). Compound **14c** was prepared in 62% yield by a procedure similar to that used to prepare compound **14a**. The title compound was obtained as a pale yellow solid (mp 91−93 °C). HPLC purity 99.5% (t_R = 27.32 min). ^{1}H NMR (600 MHz, $CDCl_3$) δ 7.22 (d, 1H, J = 8.4 Hz), 6.98 (s, 2H), 6.62 (dd, 1H, J_1 = 7.8 Hz, J_2 = 1.8 Hz), 6.14 (d, 1H, J = 2.4 Hz), 5.67 (s, 1H), 2.33 (s, 3H), 2.16 (s, 6H). ^{13}C NMR (150 MHz, $CDCl_3$) δ 143.8, 136.9, 136.5, 133.9, 133.8, 130.1, 129.6, 117.8, 117.2, 112.1, 21.1, 18.1. HRMS (ESI) calcd for $C_{15}H_{16}Cl_2N$ 280.0654 (M + H)$^+$, found 280.0656.

(4,5-Dimethylthiazol-2-yl)-(2,4,6-trimethylphenyl)amine (17). To a solution of (2,4,6-trimethylphenyl)thiourea (49 mg, 0.25 mmol) in EtOH (5 mL) was added 3-bromobutan-2-one (38 mg, 0.25 mmol). The mixture was stirred at 90 °C for 1 h. The solution was diluted with EtOAc (30 mL) and washed with H_2O (10 mL) and brine (10 mL). The organic layer was dried over Na_2SO_4 and then concentrated under reduced pressure. The residue was purified by silica gel column chromatography (hexane/EtOAc = 3/1) to give the desired product (40 mg, 65%) as a pale yellow solid (mp 180−182 °C). HPLC purity 97.5% (t_R = 22.67 min). ^{1}H NMR (600 MHz, $CDCl_3$) δ 7.70−8.00 (bs, 1H), 6.94 (s, 2H), 2.30 (s, 3H), 2.27 (s, 6H), 2.09 (s, 3H), 2.02 (s, 3H). ^{13}C NMR (150 MHz, $CDCl_3$) δ 167.4, 143.1, 137.4, 136.9, 135.5, 129.5, 113.2, 21.1, 18.2, 14.5, 11.1. HRMS (ESI) calcd for $C_{14}H_{19}N_2S$ 247.1263 (M + H)$^+$, found 247.1267.

2-Ethyl-1-(2,4,6-trimethylbenzenesulfonyl)-1*H*-pyrrole (20a). To a solution of 2-ethyl-1*H*-pyrrole (~80% purity) (24 mg, 0.25 mmol) and mesitylsulfonyl chloride (110 mg, 0.5 mmol) in 5 mL

dx.doi.org/10.1021/jm3014162 | J. Med. Chem. 2013, 56, 952−962

of THF was added 60% NaH (24 mg, 0.6 mmol) at 0 °C. The resulting mixture was stirred at room temperature for 16 h. The solution was diluted with EtOAc (50 mL), washed with 1 N HCl (aq) (10 mL) and brine (10 mL). The organic layer was dried over anhydrous Na_2SO_4 and then concentrated under reduced pressure. The residue was purified by silica gel column chromatography (hexane/EtOAc = 10/1) to give the desired product as a pale yellow solid (20 mg, 36%): mp 74−75 °C; HPLC purity 95.2% (t_R = 25.07 min). ^{1}H NMR (600 MHz, $CDCl_3$) δ 7.29−7.30 (m, 1H), 6.95 (s, 2H), 6.13−6.14 (m, 1H), 5.96−5.98 (m, 1H), 2.46 (s, 6H), 2.34−2.38 (m, 2H), 2.31 (s, 3H), 1.07 (t, 3H, J = 7.2 Hz). ^{13}C NMR (150 MHz, $CDCl_3$) δ 144.0, 140.2, 136.5, 133.5, 132.3, 122.3, 110.0, 109.1, 22.4, 21.2, 19.3, 12.4. HRMS (ESI) calcd for $C_{15}H_{20}NO_2S$ 278.1209 (M + H)$^+$, found 278.1205.

2-Ethyl-1-(toluene-4-sulfonyl)-1*H*-pyrrole (20b). Compound **20b** was prepared in 30% yield by a procedure similar to that used to prepare compound **20a**. The title compound was obtained as a colorless oil. HPLC purity 98.0% (t_R = 22.25 min). ^{1}H NMR (600 MHz, $CDCl_3$) δ 7.64 (d, 2H, J = 8.4 Hz), 7.28 (d, 2H, J = 8.4 Hz), 7.27 (d, 1H, J = 8.4 Hz), 6.20 (t, 1H, J = 3.0 Hz), 5.99 (d, 1H, J = 3.0 Hz), 2.68 (q, 2H, J = 7.2 Hz), 2.40 (s, 3H), 1.16 (t, 3H, J = 7.2 Hz). ^{13}C NMR (150 MHz, $CDCl_3$) δ 144.8, 137.5, 136.7, 130.1, 126.9, 122.4, 111.3, 111.1, 21.7, 20.6, 12.8. HRMS (ESI) calcd for $C_{13}H_{16}NO_2S$ 250.0896 (M + H)$^+$, found 250.0900.

2-Ethyl-1-(4-methoxybenzenesulfonyl)-1*H*-pyrrole (20c). Compound **20c** was prepared in 38% yield by a procedure similar to that used to prepare compound **20a**. The title compound was obtained as a pale red solid (mp 73−74 °C). HPLC purity 99.5% (t_R = 21.63 min). ^{1}H NMR (600 MHz, $CDCl_3$) δ 7.72 (d, 2H, J = 10.2 Hz), 7.28 (t, 1H, J = 1.2 Hz), 6.95 (d, 2H, J = 11.4 Hz), 6.19 (t, 1H, J = 3.0 Hz), 5.99 (d, 1H, J = 1.8 Hz), 3.85 (s, 3H), 2.69 (q, 2H, J = 7.8 Hz), 1.16 (t, 3H, J = 7.2 Hz). ^{13}C NMR (150 MHz, $CDCl_3$) δ 163.7, 137.4, 131.1, 129.2, 122.2, 114.7, 111.2, 111.0, 55.8, 20.6, 12.8. HRMS (ESI) calcd for $C_{13}H_{16}NO_3S$ 266.0845 (M + H)$^+$, found 266.0849.

1-(4-Chlorobenzenesulfonyl)-2-ethyl-1*H*-pyrrole (20d). Compound **20d** was prepared in 76% yield by a procedure similar to that used to prepare compound **20a**. The title compound was obtained as a pale red solid (mp 61−62 °C). HPLC purity 95.6% (t_R = 22.68 min). ^{1}H NMR (600 MHz, $CDCl_3$) δ 7.68 (d, 2H, J = 7.2 Hz), 7.47 (d, 2H, J = 7.2 Hz), 7.27 (d, 1H, J = 3.6 Hz), 6.23 (t, 1H, J = 3.6 Hz), 6.02 (d, 1H, J = 3.6 Hz), 2.68 (q, 2H, J = 7.2 Hz), 1.18 (t, 3H, J = 7.2 Hz). ^{13}C NMR (150 MHz, $CDCl_3$) δ 140.4, 138.1, 137.6, 129.8, 128.3, 122.4, 111.9, 111.6, 20.7, 12.8. HRMS (ESI) calcd for $C_{12}H_{13}ClNO_2S$ 271.0350 (M + H)$^+$, found 270.0355.

2-Ethyl-1-(4-trifluoromethyl-benzenesulfonyl)-1*H*-pyrrole (20e). Compound **20e** was prepared in 58% yield by a procedure similar to that used to prepare compound **20a**. The title compound was obtained as a pale red solid (mp 55−57 °C). HPLC purity 96.0% (t_R = 22.82 min). ^{1}H NMR (600 MHz, $CDCl_3$) δ 7.86 (d, 2H, J = 7.8 Hz), 7.76 (d, 2H, J = 7.8 Hz), 7.28−2.30 (m, 1H), 6.25 (d, 1H, J = 1.8 Hz), 6.03−6.05 (m, 1H), 2.68 (q, 2H, J = 7.2 Hz), 1.18 (t, 3H, J = 7.8 Hz). HRMS (ESI) calcd for $C_{13}H_{13}F_3NO_2S$ 304.0614 (M + H)$^+$, found 304.0602.

2-Ethyl-1-(toluene-2-sulfonyl)-1*H*-pyrrole (20f). Compound **20f** was prepared in 73% yield by a procedure similar to that used to prepare compound **20a**. The title compound was obtained as a pale red oil (mp 55−57 °C). HPLC purity 98.3% (t_R = 22.42 min). ^{1}H NMR (600 MHz, $CDCl_3$) δ 7.50 (d, 2H, J = 7.2 Hz), 7.31−7.36 (m, 3H), 6.24−6.26 (m, 1H), 6.07−6.09 (m, 1H), 2.55 (q, 2H, J = 7.2 Hz), 2.54 (s, 3H), 1.13 (t, 3H, J = 7.2 Hz). ^{13}C NMR (150 MHz, $CDCl_3$) δ 138.6, 138.0, 137.6, 133.7, 132.9, 128.3, 126.5, 123.0, 110.7, 110.3, 20.3, 20.0, 12.6. HRMS (ESI) calcd for $C_{13}H_{16}NO_2S$ 250.0896 (M + H)$^+$, found 250.0900.

1-(3,5-Dimethylbenzenesulfonyl)-2-ethyl-1*H*-pyrrole (20g). Compound **20g** was prepared in 67% yield by a procedure similar to that used to prepare compound **20a**. The title compound was obtained as a pale red solid (mp 67−70 °C). HPLC purity 98.2% (t_R = 23.09 min). ^{1}H NMR (600 MHz, $CDCl_3$) δ 7.36 (s, 2H), 7.29 (s, 1H), 7.19 (s, 1H), 6.21 (t, 1H, J = 3.0 Hz), 6.00 (s, 1H), 2.70 (q, 2H, J = 7.2 Hz), 2.35 (s, 6H), 1.17 (t, 3H, J = 7.2 Hz). ^{13}C NMR (150 MHz, $CDCl_3$) δ 139.6, 139.4, 137.5, 135.5, 124.3, 122.4, 111.2, 111.0, 21.4, 20.6, 12.9. HRMS (ESI) calcd for $C_{14}H_{18}NO_2S$ 264.1053 (M + H)$^+$, found 264.1056.

1-(2,4-Dimethylbenzenesulfonyl)-2-ethyl-1*H*-pyrrole (20h). Compound **20h** was prepared in 76% yield by a procedure similar to that used to prepare compound **20a**. The title compound was obtained as a white solid (mp 75−77 °C). HPLC purity 98.3% (t_R = 24.40 min). ^{1}H NMR (600 MHz, $CDCl_3$) δ 7.46 (d, 1H, J = 7.2 Hz), 7.33−7.35 (m, 1H), 7.10−7.12 (m, 2H), 6.22−6.24 (m, 1H), 6.04−6.06 (m, 1H), 2.55 (q, 2H, J = 7.2 Hz), 2.47 (s, 3H), 2.39 (s, 3H), 1.13 (t, 3H, J = 7.2 Hz). ^{13}C NMR (150 MHz, $CDCl_3$) δ 144.7, 137.9, 137.4, 135.5, 133.6, 128.7, 127.1, 122.9, 110.6, 110.1, 21.4, 20.3, 19.8, 12.6. HRMS (ESI) calcd for $C_{14}H_{18}NO_2S$ 264.1053 (M + H)$^+$, found 264.1058.

2,4-Dimethyl-1-(2,4,6-trimethylbenzenesulfonyl)-1*H*-pyrrole (20i). Compound **20i** was prepared in 58% yield by a procedure similar to that used to prepare compound **20a**. The title compound was obtained as a pale red solid (mp 98−100 °C). HPLC purity 95.7% (t_R = 25.20 min). ^{1}H NMR (600 MHz, $CDCl_3$) δ 7.01 (s, 1H), 6.95 (s, 2H), 5.77 (s, 1H), 2.49 (s, 6H), 2.31 (s, 3H), 2.00 (s, 3H), 1.99 (s, 3H). ^{13}C NMR (150 MHz, $CDCl_3$) δ 143.8, 140.2, 133.8, 132.2, 130.2, 119.7, 119.2, 114.5, 23.4, 21.1, 12.6, 11.8. HRMS (ESI) calcd for $C_{15}H_{20}NO_2S$ 278.1209 (M + H)$^+$, found 278.1205.

1-(2,4,6-Trimethylbenzenesulfonyl)-1*H*-indole (22a). Compound **22a** was prepared in 84% yield by a procedure similar to that used to prepare compound **20a**. The title compound was obtained as a white solid (mp 110−112 °C). HPLC purity 98.9% (t_R = 24.73 min). ^{1}H NMR (600 MHz, $CDCl_3$) δ 7.59−7.61 (m, 1H), 7.54−7.55 (m, 1H), 7.34−7.35 (m, 1H), 7.17 (s, 2H), 6.93 (s, 2H), 6.61−6.62 (m, 1H), 2.52 (s, 6H), 2.26 (s, 3H). ^{13}C NMR (150 MHz, $CDCl_3$) δ 144.1, 140.3, 134.7, 133.1, 132.5, 130.3, 126.8, 124.2, 122.8, 121.5, 112.5, 106.5, 22.7, 21.1. HRMS (ESI) calcd for $C_{17}H_{18}NO_2S$ 300.1053 (M + H)$^+$, found 300.1057.

1-(2,4,6-Trimethylbenzenesulfonyl)-1*H*-indole-5-carboxylic Acid Methyl Ester (22b). Compound **22b** was prepared in 84% yield by a procedure similar to that used to prepare compound **20a**. The title compound was obtained as a white solid (mp 131−133 °C). HPLC purity 99.4% (t_R = 23.80 min). ^{1}H NMR (600 MHz, $CDCl_3$) δ 8.30 (s, 1H), 7.88 (d, 1H, J = 9.0 Hz), 7.64 (d, 1H, J = 3.6 Hz), 7.40 (d, 1H, J = 8.4 Hz), 6.95 (s, 2H), 6.70 (d, 1H, J = 3.6 Hz), 3.90 (s, 3H), 2.51 (s, 6H), 2.28 (s, 3H). ^{13}C NMR (150 MHz, $CDCl_3$) δ 167.3, 144.6, 140.4, 137.3, 132.8, 132.6, 130.0, 128.0, 125.6, 125.1, 123.9, 112.3, 107.1, 52.2, 22.7, 21.2. HRMS (ESI) calcd for $C_{19}H_{20}NO_4S$ 358.1108 (M + H)$^+$, found 358.1114.

1-(2,4,6-Trimethylbenzenesulfonyl)-1*H*-indole-5-carboxylic Acid (22c). To a solution of **22b** (72 mg, 0.2 mmol) in MeOH/H_2O (4 mL/1 mL) was added 2 N LiOH (0.4 mL, 0.8 mmol). The mixture was stirred at room temperature for 16 h. The solution was diluted with EtOAc (30 mL), washed with 1 N HCl (aq) (10 mL) and brine (10 mL). The organic layer was dried over Na_2SO_4 and then concentrated under reduced pressure. The residue was purified by silica gel column chromatography (hexane/EtOAc = 1/1) to give the desired product (45 mg, 66%) as a pale yellow solid (mp 223−224 °C). HPLC purity 98.4% (t_R = 14.89 min). ^{1}H NMR (600 MHz, DMSO-d_6) δ 12.80 (bs, 1H), 8.28 (s, 1H), 7.83−7.86 (m, 2H), 7.40 (d, 1H, J = 8.4 Hz), 7.15 (m, 2H), 6.94 (d, 1H, J = 3.6 Hz), 2.44 (s, 6H), 2.27 (s, 3H). ^{13}C NMR (150 MHz, DMSO-d_6) δ 167.3, 144.7, 139.6, 136.3, 132.5, 131.9, 129.7, 128.5, 125.6, 125.4, 123.7, 111.8, 107.6, 21.9, 20.5. HRMS (ESI) calcd for $C_{18}H_{18}NO_4S$ 344.0951 (M + H)$^+$, found 344.0954.

1-(2,4,6-Trimethylbenzenesulfonyl)-1*H*-pyrrolo[3,2-*b*]-pyridine (24a). Compound **24a** was prepared in 96% yield by a procedure similar to that used to prepare compound **20a**. The title compound was obtained as a white solid (mp 105−107 °C). HPLC purity 99.8% (t_R = 21.84 min). ^{1}H NMR (600 MHz, $CDCl_3$) δ 8.48 (d, 1H, J = 3.6 Hz), 7.74−7.75 (m, 1H), 7.71 (d, 1H, J = 8.4 Hz), 7.09−7.11 (m, 1H), 6.94 (s, 2H), 6.81 (d, 1H, J = 3.0 Hz), 2.50 (s, 6H), 2.25 (s, 3H). ^{13}C NMR (150 MHz, $CDCl_3$) δ 148.1, 145.8, 144.7, 140.4, 132.6, 132.5, 129.6, 128.3, 119.8, 118.7, 107.8, 22.7, 21.1.

dx.doi.org/10.1021/jm3014162 | J. Med. Chem. 2013, 56, 952−962

HRMS (ESI) calcd for $C_{16}H_{17}N_2O_2S$ 301.1005 $(M + H)^+$, found 301.1010.

1-(2,4,6-Trimethylbenzenesulfonyl)-1*H*-pyrrolo[3,2-*c*]-pyridine (24b). Compound **24b** was prepared in 84% yield by a procedure similar to that used to prepare compound **20a**. The title compound was obtained as a white solid (mp 119−120 °C). HPLC purity 99.7% (t_R = 22.77 min). ^{1}H NMR (600 MHz, $CDCl_3$) δ 8.88 (s, 1H), 8.33 (d, 1H, J = 6.0 Hz), 7.54 (d, 1H, J = 3.6 Hz), 7.29 (d, 1H, J = 5.4 Hz), 6.95 (s, 2H), 6.68 (d, 1H, J = 3.6 Hz), 2.50 (s, 6H), 2.26 (s, 3H). ^{13}C NMR (150 MHz, $CDCl_3$) δ 144.8, 144.3, 143.6, 140.4, 139.0, 132.6, 132.3, 127.2, 126.4, 107.6, 105.1, 22.6, 21.1. HRMS (ESI) calcd for $C_{16}H_{17}N_2O_2S$ 301.1005 $(M + H)^+$, found 301.1009.

1-(2,4,6-Trimethylbenzenesulfonyl)-1*H*-pyrrolo[2,3-*c*]-pyridine (24c). Compound **24c** was prepared in 87% yield by a procedure similar to that used to prepare compound **20a**. The title compound was obtained as a white solid (mp 132−134 °C). HPLC purity 99.8% (t_R = 21.77 min). ^{1}H NMR (600 MHz, $CDCl_3$) δ 8.69 (s, 1H), 8.35 (d, 1H, J = 5.4 Hz), 7.73 (d, 1H, J = 3.6 Hz), 7.48 (d, 1H, J = 5.4 Hz), 6.96 (s, 2H), 6.63 (d, 1H, J = 3.0 Hz), 2.53 (s, 6H), 2.28 (s, 3H). ^{13}C NMR (150 MHz, $CDCl_3$) δ 144.9, 142.1, 140.6, 135.8, 135.1, 132.8, 132.4, 131.8, 130.0, 115.9, 105.5, 22.7, 21.2. HRMS (ESI) calcd for $C_{16}H_{17}N_2O_2S$ 301.1005 $(M + H)^+$, found 301.1011.

1-(2,4,6-Trimethylbenzenesulfonyl)-1*H*-pyrrolo[2,3-*b*]-pyridine (24d). Compound **24d** was prepared in 87% yield by a procedure similar to that used to prepare compound **20a**. The title compound was obtained as a white solid (mp 139−141 °C). HPLC purity 99.6% (t_R = 22.81 min). ^{1}H NMR (600 MHz, $CDCl_3$) δ 8.22 (d, 1H, J = 4.2 Hz), 7.85 (d, 1H, J = 3.0 Hz), 7.83 (d, 1H, J = 7.8 Hz), 7.08−7.11 (m, 1H), 6.93 (s, 2H), 6.57 (d, 1H, J = 3.0 Hz), 2.71 (s, 6H), 2.27 (s, 3H). ^{13}C NMR (150 MHz, $CDCl_3$) δ 147.6, 144.7, 144.0, 141.3, 132.8, 132.1, 129.3, 126.9, 122.4, 118.6, 103.8, 23.0, 21.2. HRMS (ESI) calcd for $C_{16}H_{17}N_2O_2S$ 301.1005 $(M + H)^+$, found 301.0981.

Biological Evaluation Methods. Primary Screen Assay. Fluorescence intensity of 8-NBD-cAMP in complex with EPAC2 has been used as the readout in the primary screen assay. Briefly, 50 nM EPAC2 solution was prepared in 20 mM Tris buffer, pH 7.5, containing 150 mM NaCl, 1 mM EDTA, and 1 mM DDT. 8-NBD-cAMP was added to EPAC2 solution up to 60 nM from stock solution in water. Sample was dispensed into 96-well plate (100 μL/well), and test compounds were added (1 μL/well) from 96-well mother plates. Test compounds were added from 10 mM stock solutions in DMSO. Samples with cAMP addition (1 μL/well from 30 mM stock solution in water) and no additions were used as a positive and a negative control. Fluorescence intensity signal from 8-NBD probe was recorded at room temperature before and after tested compounds were added using SpectraMaxM2 microplate reader (Molecular Devices, Silicon Valley, CA, U.S.) with excitation/emission wavelengths set at 470/540 nm.

Secondary Confirmation Assay. Measurement of in vitro guanine nucleotide exchange factor (GEF) activity of EPAC was adapted from a well-known fluorescence-based assay using a fluorescent guanine nucleotide analogue[30] and used as a functional confirmation assay for the compounds identified from primary screen. Briefly, 0.2 μM Rap1B (1−167) loaded with the fluorescent GDP analogue (Mant-GDP) was incubated with EPAC in 50 mM Tris buffer, pH 7.5, containing 50 mM NaCl, 5 mM $MgCl_2$, 1 mM DTT, and a 100-fold molar excess of unlabeled GDP (20 μM) in the presence of 25 μM tested compound and 25 μM cAMP. Exchange of Mant-GDP by GDP was measured as a decrease in fluorescence intensity over time using a FluoroMax-3 spectrofluorometer with excitation/emission wavelengths set at 366/450 nm. Typically, decay in the fluorescence intensity was recorded over a time course of 6000 s with data points taken every 60 s.

Counter Screening Assay. Kinase activities of the type I and type II PKA holoenzymes were measured spectrophotometrically in a 96-well plate with a coupled enzyme assay as described previously.[31] In this assay, the formation of the ADP is coupled to the oxidation of NADH by the pyruvate kinase/lactate dehydrogenase reactions so the reaction rate can be determined by following the oxidation of NADH, reflected by a decrease in absorbance at 340 nm. The kinase reaction mixture (100 μL) contained 50 mM Mops (pH 7.0), 10 mM $MgCl_2$, 1 mM ATP, 1 mM PEP, 0.1 mM NADH, 8 U of pyruvate kinase, 15 U of lactate dehydrogenase, a fixed amount of type I or type II PKA holoenzyme, and 0.1 mM cAMP, with or without 25 μM test compound. Reactions were pre-equilibrated at room temperature and initiated by adding the kemptide substrate (final concentration, 0.26 mM). PKA activities measured in the presence of 25 μM H89, a selective PKA inhibitor, were used as positive controls of PKA inhibition.

FRET-Based Assay for EPAC1, EPAC2, or AKAR3 Activation. HEK293 cells stably transfected with genetically encoded FRET biosensors for EPAC1 (EPAC1 FL), EPAC2 (EPAC2 FL), or PKA (AKAR3) were used in this study. EPAC1 FL and EPAC2 FL were generated by sandwiching the full-length human EPAC1 or EPAC2 proteins with a Cerulean variant of cyan fluorescent protein (CFP) at their N-termini and a Venus variant of yellow fluorescent protein (YFP) at their C-termini.[23] Activation of EPAC1 or EPAC2 in response to cAMP was measured as a decrease of FRET, and it was plotted as an increase of the CFP/YFP emission ratio (i.e., 485/535 nm emission ratio). The function core of AKAR3 contains a PKA substrate motif and a phosphoamino acid binding domain connected by a flexible linker, which is flanked by a variant of CFP at its N-terminus and a variant of YFP at its C-terminus.[24] Activation of AKAR3 in response to cAMP was measured as an increase of FRET, and it was plotted as a decrease of the 485/535 nm emission ratio. To test the effect of **20i** on EPAC1, EPAC2, or PKA activation in live cells, single-cell suspensions of EPAC1-C9, EPAC2-C1, and AKAR3-C12 clones were plated onto 96-well clear-bottom assay plates (Costar 3904) coated with rat tail collagen (Invitrogen). The clones were maintained in DMEM (25 mM glucose, 10% FBS) for 24 h in order to allow the cell cultures to become 80−90% confluent. Cells were pretreated with various concentrations of **20i** or vehicle control before being activated by membrane permeable cAMP analogues. Fluorescence spectra were recorded as described previously[32] using a FlexStation 3 microplate reader controlled using SoftMax Pro software (Molecular Devices) with the excitation wavelength set at 435/9 nm (455 nm cutoff) and the emission wavelength set at 485/15 nm (CFP) or 535/15 nm (YFP). The time course of the change of FRET ratio was plotted after exporting data to Origin, version 7.5 (OriginLab).

■ ASSOCIATED CONTENT

Supporting Information

^{1}H and ^{13}C NMR spectra of all new compounds. This material is available free of charge via the Internet at http://pubs.acs.org.

■ AUTHOR INFORMATION

Corresponding Author

*For X.C.: phone, (409) 772-9656; fax, (409) 772-7050; e-mail, xcheng@utmb.edu. For J.Z.: phone, (409) 772-9748; fax, (409) 772-9818; e-mail, jizhou@utmb.edu.

Notes

The authors declare no competing financial interest.

■ ACKNOWLEDGMENTS

This work was supported by Grants P30DA028821, R21MH093844 (J.Z.), R01GM066170, and R21NS066510 (X.C.) from the National Institutes of Health, R. A. Welch Foundation Chemistry and Biology Collaborative Grant from Gulf Coast Consortia (GCC) for Chemical Genomics, and John Sealy Memorial Endowment Fund. We thank Dr. Jin Zhang of Johns Hopkins School of Medicine for providing the EPAC1, EPAC2, and AKAR3 FRET reporters. We also thank Drs. Lawrence C. Sowers, Carol L. Nilsson, Jacob A. Theruvathu, and Huiling Liu for mass spectrometry assistance

and Dr. Tianzhi Wang at the NMR core facility of University of Texas Medical Branch for the NMR spectroscopy assistance.

■ ABBREVIATIONS USED

EPAC, exchange proteins directly activated by cAMP; SAR, structure−activity relationship; cAMP, cyclic adenosine monophosphate; 8-NBD-cAMP, 8-(2-[7-nitro-4-benzofurazanyl]-aminoethylthio)adenosine 3′,5′-cyclic monophosphate; GDP, guanosine diphosphate; PKA, protein kinase A; FRET, fluorescence resonance energy transfer; GEF, guanine nucleotide exchange factor; GTP, guanosine triphosphate; Rap, Ras-related protein; HTS, high-throughput screening; 007-AM, 8-(4-chlorophenylthio)-2′-*O*-methyladenosine 3′,5′-cyclic monophosphate acetoxymethyl ester; AKAR3, A-kinase activity reporter 3; 8-Br-cAMP-AM, 8-bromoadenosine 3′,5′-cyclic monophosphate acetoxymethyl ester; TLC, thin layer chromatography; UV, ultraviolet; TMS, tetramethylsilane; HRMS, high-resolution mass spectrometry; HPLC, high-performance liquid chromatography; TFA, trifluoroacetic acid; DCM, dichloromethane; EtOAc, ethyl acetate; DMSO, dimethyl sulfoxide; EDTA, ethylenediaminetetraacetic acid; DDT, dichlorodiphenyltrichloroethane; ADP, adenosine diphosphate; NADH, nicotinamide adenine dinucleotide; PEP, phospho-(enol)pyruvate; H89, *N*-[2-[[3-(4-bromophenyl)-2-propenyl]-amino]ethyl]-5-isoquinolinesulfonamide dihydrochloride; CFP, cyan fluorescent protein; YFP, yellow fluorescent protein; DMEM, Dulbecco's modified Eagle medium; FBS, fetal bovine serum

■ REFERENCES

(1) Frye, S. V. The art of the chemical probe. *Nat. Chem. Biol.* **2010**, *6*, 159−161.
(2) Beavo, J. A.; Brunton, L. L. Cyclic nucleotide research—still expanding after half a century. *Nat. Rev. Mol. Cell Biol.* **2002**, *3*, 710−718.
(3) de Rooij, J.; Zwartkruis, F. J.; Verheijen, M. H.; Cool, R. H.; Nijman, S. M.; Wittinghofer, A.; Bos, J. L. EPAC is a Rap1 guanine-nucleotide-exchange factor directly activated by cyclic AMP. *Nature* **1998**, *396*, 474−477.
(4) Kawasaki, H.; Springett, G. M.; Mochizuki, N.; Toki, S.; Nakaya, M.; Matsuda, M.; Housman, D. E.; Graybiel, A. M. A family of cAMP-binding proteins that directly activate Rap1. *Science* **1998**, *282*, 2275−2279.
(5) Bos, J. L. EPAC: a new cAMP target and new avenues in cAMP research. *Nat. Rev. Mol. Cell Biol.* **2003**, *4*, 733−738.
(6) Cheng, X.; Ji, Z.; Tsalkova, T.; Mei, F. C. EPAC and PKA: a tale of two intracellular cAMP receptors. *Acta Biochim. Biophys. Sin.* **2008**, *40*, 651−662.
(7) Bos, J. L. EPAC proteins: multi-purpose cAMP targets. *Trends Biochem. Sci.* **2006**, *31*, 680−686.
(8) Gloerich, M.; Bos, J. L. EPAC: defining a new mechanism for cAMP action. *Annu. Rev. Pharmacol. Toxicol.* **2010**, *50*, 355−375.
(9) Grandoch, M.; Roscioni, S. S.; Schmidt, M. The role of EPAC proteins, novel cAMP mediators, in the regulation of immune, lung and neuronal function. *Br. J. Pharmacol.* **2010**, *159*, 265−284.
(10) Breckler, M.; Berthouze, M.; Laurent, A. C.; Crozatier, B.; Morel, E.; Lezoualc'h, F. Rap-linked cAMP signaling EPAC proteins: compartmentation, functioning and disease implications. *Cell. Signalling* **2011**, *23*, 1257−1266.
(11) (a) Holz, G. G.; Kang, G.; Harbeck, M.; Roe, M. W.; Chepurny, O. G. Cell physiology of cAMP sensor EPAC. *J. Physiol.* **2006**, *577*, 5−15. (b) Holz, G. G; Chepurny, O. G; Schwede, F. EPAC-selective cAMP analogs: new tools with which to evaluate the signal transduction properties of cAMP-regulated guanine nucleotide exchange factors. *Cell Signalling* **2008**, *20*, 10−20.
(12) Rehmann, H.; Schwede, F.; Døskeland, S. O.; Wittinghofer, A.; Bos, J. L. Ligand-mediated activation of the cAMP-responsive guanine nucleotide exchange factor EPAC. *J. Biol. Chem.* **2003**, *278*, 38548−38556.
(13) Dao, K. K.; Teigen, K.; Kopperud, R.; Hodneland, E.; Schwede, F.; Christensen, A. E.; Martinez, A.; Døskeland, S. O. EPAC1 and cAMP-dependent protein kinase holoenzyme have similar cAMP affinity, but their cAMP domains have distinct structural features and cyclic nucleotide recognition. *J. Biol. Chem.* **2006**, *281*, 21500−21511.
(14) Das, R.; Chowdhury, S.; Mazhab-Jafari, M. T.; Sildas, S.; Selvaratnam, R.; Melacini, G. Dynamically driven ligand selectivity in cyclic nucleotide binding domains. *J. Biol. Chem.* **2009**, *284*, 23682−23696.
(15) Selvaratnam, R.; Chowdhury, S.; VanSchouwen, B.; Melacini, G. Mapping allostery through the covariance analysis of NMR chemical shifts. *Proc. Natl. Acad. Sci. U.S.A.* **2011**, *108*, 6133−6138.
(16) Tsalkova, T.; Mei, F. C.; Cheng, X. A fluorescence-based high-throughput assay for the discovery of exchange protein directly activated by cyclic AMP (EPAC) antagonists. *PLoS One* **2012**, *7*, e30441.
(17) Chen, H.; Tsalkova, T.; Mei, F. C.; Hu, Y.; Cheng, X.; Zhou, J. 5-Cyano-6-oxo-1,6-dihydro-pyrimidines as potent antagonists targeting exchange proteins directly activated by cAMP. *Bioorg. Med. Chem. Lett.* **2012**, *22*, 4038−4043.
(18) (a) Almahariq, M.; Tsalkova, T.; Mei, F. C.; Chen, H.; Zhou, J.; Sastry, S. K.; Schwede, F.; Cheng, X. A novel EPAC specific inhibitor suppresses pancreatic cancer cell migration and invasion. *Mol. Pharmacol.* **2013**, *83*, 122−128. (b) Tsalkova, T.; Mei, F. C.; Li, S.; Chepurny, O. G.; Leech, C. A.; Liu, T.; Holz, G. G.; Woods, V. L., Jr.; Cheng, X. Isoform-specific antagonists of exchange proteins directly activated by cAMP. *Proc. Natl. Acad. Sci. U.S.A.* **2012**, *109*, 18613−18618.
(19) Tsalkova, T.; Blumenthal, D. K.; Mei, F. C.; White, M. A.; Cheng, X. Mechanism of EPAC activation: structural and functional analyses of EPAC2 hinge mutants with constitutive and reduced activities. *J. Biol. Chem.* **2009**, *284*, 23644−23651.
(20) Li, S.; Tsalkova, T.; White, M. A.; Mei, F. C.; Liu, T.; Wang, D.; Woods, V. L., Jr.; Cheng, X. Mechanism of intracellular cAMP sensor EPAC2 activation: cAMP-induced conformational changes identified by amide hydrogen/deuterium exchange mass spectrometry (DXMS). *J. Biol. Chem.* **2011**, *286*, 17889−17897.
(21) Cheng, X.; Phelps, C.; Taylor, S. S. Differential binding of cAMP-dependent protein kinase regulatory subunit isoforms Ialpha and IIbeta to the catalytic subunit. *J. Biol. Chem.* **2001**, *276*, 4102−4108.
(22) Yu, S.; Mei, F. C.; Lee, J. C.; Cheng, X. Probing cAMP-dependent protein kinase holoenzyme complexes I alpha and II beta by FT-IR and chemical protein footprinting. *Biochemistry* **2004**, *43*, 1908−1920.
(23) Herbst, K. J.; Coltharp, C.; Amzel, L. M.; Zhang, J. Direct activation of EPAC by sulfonylurea is isoform selective. *Chem. Biol.* **2011**, *18*, 243−251.
(24) Allen, M. D.; Zhang, J. Subcellular dynamics of protein kinase A activity visualized by FRET-based reporters. *Biochem. Biophys. Res. Commun.* **2006**, *348*, 716−721.
(25) Holz, G. G. EPAC: a new cAMP-binding protein in support of glucagon-like peptide-1 receptor-mediated signal transduction in the pancreatic beta-cell. *Diabetes* **2004**, *53*, 5−13.
(26) Zhang, C. L.; Katoh, M.; Shibasaki, T.; Minami, K.; Sunaga, Y.; Takahashi, H.; Yokoi, N.; Iwasaki, M.; Miki, T.; Seino, S. The cAMP sensor EPAC2 is a direct target of antidiabetic sulfonylurea drugs. *Science* **2009**, *325*, 607−610.
(27) Morel, E.; Marcantoni, A.; Gastineau, M.; Birkedal, R.; Rochais, F.; Garnier, A.; Lompre, A. M.; Vandecasteele, G.; Lezoualc'h, F. cAMP-binding protein EPAC induces cardiomyocyte hypertrophy. *Circ. Res.* **2005**, *97*, 1296−1304.
(28) Metrich, M.; Lucas, A.; Gastineau, M.; Samuel, J. L.; Heymes, C.; Morel, E.; Lezoualc'h, F. EPAC mediates beta-adrenergic receptor-induced cardiomyocyte hypertrophy. *Circ. Res.* **2008**, *102*, 959−965.

(29) Lissitzky, J. C.; Parriaux, D.; Ristorcelli, E.; Verine, A.; Lombardo, D.; Verrando, P. Cyclic AMP signaling as a mediator of vasculogenic mimicry in aggressive human melanoma cells in vitro. *Cancer Res.* **2009**, *69*, 802−809.
(30) van den Berghe, N.; Cool, R. H.; Horn, G.; Wittinghofer, A. Biochemical characterization of C3G: an exchange factor that discriminates between Rap1 and Rap2 and is not inhibited by Rap1A(S17N). *Oncogene* **1997**, *15*, 845−850.
(31) Cook, P. F.; Neville, M. E., Jr.; Vrana, K. E.; Hartl, F. T.; Roskoski, R., Jr. Adenosine cyclic 3′,5′-monophosphate dependent protein kinase: kinetic mechanism for the bovine skeletal muscle catalytic subunit. *Biochemistry* **1982**, *21*, 5794−5799.
(32) Chepurny, O. G.; Leech, C. A.; Kelley, G. G.; Dzhura, I.; Dzhura, E.; Li, X.; Rindler, M. J.; Schwede, F.; Genieser, H. G.; Holz, G. G. Enhanced Rap1 activation and insulin secretagogue properties of an acetoxymethyl ester of an EPAC-selective cyclic AMP analog in rat INS-1 cells: studies with 8-pCPT-2′-O-Me-cAMP-AM. *J. Biol. Chem.* **2009**, *284*, 10728−10736.

■ NOTE ADDED AFTER ASAP PUBLICATION

After this paper was published ASAP on January 15, 2013, a correction was made to the Acknowledgments. The revised version was reposted January 31, 2013.